Chaotic background of large-scale climate oscillations

A. Bershadskii
ICAR, P.O.B. 31155, Jerusalem 91000, Israel

It is shown that the periodic alteration of night and day provides a chaotic dissipation mechanism for the North Atlantic (NAO) and Southern (SOI) climate oscillations. The wavelet regression detrended daily NAO index for last 60 years and daily SOI for last 20 years as well as an analytical continuation in the complex time domain were used for this purpose.

PACS numbers: 05.45.Gg, 92.60.Ry, 92.70.Qr

It is now well known that climate is a nonlinear system, which can exhibit a chaotic behavior. Therefore, the climate response to the periodic forcing does not always have the result that one might expect. Already pioneering studies of the effect of external periodic forcing on the first Lorenz model of the chaotic climate revealed very interesting properties of chaotic response (see, for instance, [1],[2]). Unlike linear systems, where periodic forcing leads to periodic response, nonlinear chaotic response to periodic forcing can result in exponentially *decaying* broad-band power spectrum [3]-[7]. Thus, the chaotic response to periodic forcing can provide a *dissipation* mechanism for the considered system, especially in the case when the system's pumping frequency is considerably lower than the frequency of the periodic forcing under consideration. The climate, where the chaotic behavior was discovered for the first time, is still one of the most challenging areas for the chaotic response theory. The weather (time scales up to several weeks) chaotic behavior usually can be directly related to chaotic convection, while appearance of the chaotic properties for more long-term climate events is a non-trivial and challenging phenomenon (see for instance, recent Ref. [7] and references therein).

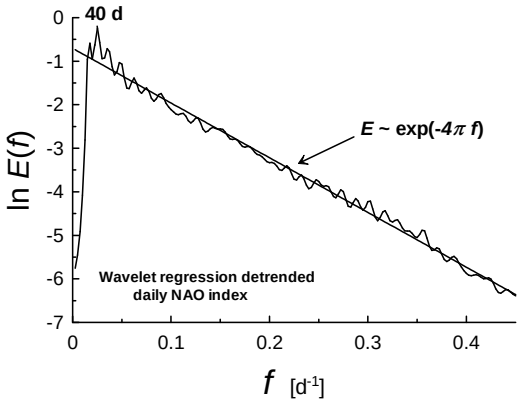

FIG. 1: Spectrum of the wavelet regression detrended NAO data series (the NAO index data were taken from Ref. [9]). In the semi-logarithmic scales used in the figure the straight line indicates the exponential decay Eq. (1).

"And in the alteration of night and day, and the food We send down from the sky, and revives therewith the earth after its death, and in the turning about of winds are signs for people of understanding". QURAN (45:4-5).

The solar day is a period of time during which the earth makes one revolution on its axis relative to the sun. During a part of the day the sun's direct rays are blocked (locally) by the earth. Therefore, the periodic *daily* variability of solar impact plays crucial role in high frequency climate behavior. It will be shown in present paper that just unusual properties of *chaotic* response to the daily periodicity of solar forcing provide an effective mechanism for high frequency dissipation of the large-scale climate oscillations.

One of the most significant and recurrent patterns of atmospheric variability over the middle and high latitudes of the Northern Hemisphere is known as NAO - North Atlantic Oscillation. Climate variability from the subtropical Atlantic to the Arctic and from Siberia to the eastern boards of the North America is strongly related to the NAO (see, for a recent comprehensive review Ref. [8]). In Ref. [9] a projection of the daily 500mb height anomalies over the Northern Hemisphere onto the loading pattern [10] of the NAO was used in order to construct the daily NAO for last 60 years. Due to the natural climatic trends the daily NAO index time series is not a statistically stationary data set. In order to solve this problem a wavelet regression detrending method was used in present investigation for the daily NAO time series [11]. We used a symmlet regression of the data. Most of the regression methods are linear in responses. At the nonlinear nonparametric wavelet regression one chooses a relatively small number of wavelet coefficients to represent the underlying regression function. A threshold method is used to keep or kill the wavelet coefficients. In this case, in particular, the Universal (VisuShrink) thresholding rule with a soft thresholding function was used. At the wavelet regression the demands to smoothness of the function being estimated are relaxed considerably in comparison to the traditional methods. Figure 1 shows a spectrum of the wavelet regression detrended

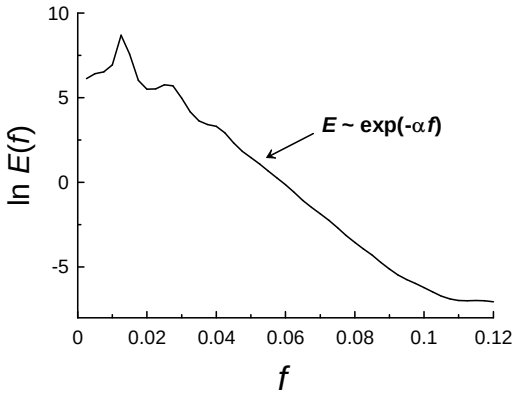

FIG. 2: As in Fig.1 but for z-component of the Lorenz chaotic attractor Eq. (2). In the semi-logarithmic scales used in the figure the straight line indicates the exponential decay.

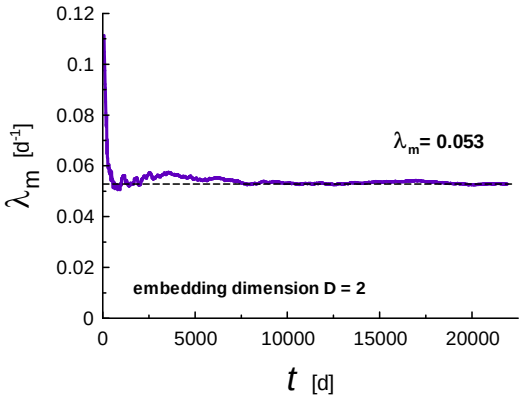

FIG. 3: The pertaining average maximal Lyapunov exponent at the pertaining time, calculated for the same data as those used for calculation of the spectrum (Fig. 1). The dashed straight line indicates convergence to a positive value.

data [9] calculated using the maximum entropy method because it provides an optimal spectral resolution even for small data sets. The spectrum exhibits a broad-band behavior with exponential decay:

$$E(f) \sim e^{-4\pi f} \tag{1}$$

A semi-logarithmic plot was used in Fig. 1 in order to show the exponential decay (at this plot the exponential decay corresponds to a straight line, for an explanation see below).

Both stochastic and deterministic processes can result in the broad-band part of the spectrum, but the decay in the spectral power is different for the two cases. The exponential decay indicates that the broad-band spectrum for these data arises from a deterministic rather than a stochastic process. For a wide class of deterministic systems a broad-band spectrum with exponential decay is a generic feature of their chaotic solutions Refs. [3]-[5]. Let us consider a relevant example. The Lorenz equations are given by:

$$\frac{dx}{dt} = \sigma(y-x), \quad \frac{dy}{dt} = rx - y - xz, \quad \frac{dz}{dt} = xy - bz \tag{2}$$

The standard values producing a chaotic attractor are: $\sigma = 10.0,\ r = 28.0,\ b = 8/3$. Figure 2 shows a power spectrum for z-component of the Lorenz chaotic attractor generated by Eq. (2) (the spectrum was again calculated using the maximum entropy method). A semi-logarithmic plot was used again in Fig. 2 in order to show exponential decay (at this plot the exponential decay corresponds to a straight line). Nature of the exponential decay of the power spectra of the chaotic systems is still an unsolved mathematical problem. A progress in solution of this problem has been achieved by the use of the analytical continuation of the equations in the complex domain (see, for instance, [6]). In this approach the exponential decay of chaotic spectrum is related to a singularity in the plane of complex time, which lies nearest to the real axis. Distance between this singularity and the real axis determines the rate of the exponential decay. For many interesting cases chaotic solutions are analytic in a finite strip around the real time axis. This takes place, for instance for attractors bounded in the real domain (the Lorenz attractor, for instance). In this case the radius of convergence of the Taylor series is also bounded (uniformly) at any real time. Let us consider, for simplicity, solution $u(t)$ with simple poles only, and to define the Fourier transform as follows

$$u(\omega) = (2\pi)^{-1/2} \int_{-T_e/2}^{T_e/2} dt\ e^{-i\omega t} u(t) \tag{3}$$

Then using the theorem of residues

$$u(\omega) = i(2\pi)^{1/2} \sum_j R_j \exp(i\omega x_j - |\omega y_j|) \tag{4}$$

where R_j are the poles residue and $x_j + iy_j$ are their location in the relevant half plane, one obtains asymptotic behavior of the spectrum $E(\omega) = |u(\omega)|^2$ at large ω

$$E(f) \sim \exp(-4\pi f\ y_{min}) \tag{5}$$

where $\omega = 2\pi f$ and y_{min} is the imaginary part of the location of the pole which lies nearest to the real axis. If in the considered case $y_{min} = 1$d, than we obtain the exponential decay shown in Fig. 1 (cf Eq. (1)). In order to understand the reason for $y_{min} = 1$d we need in a nonlinear dynamic climate model where the *daily* periodic solar impact results in such position of the pole nearest to the real axis. But even before constructing such dynamic model it is already clear that just the *daily* periodicity of the solar impact is responsible for

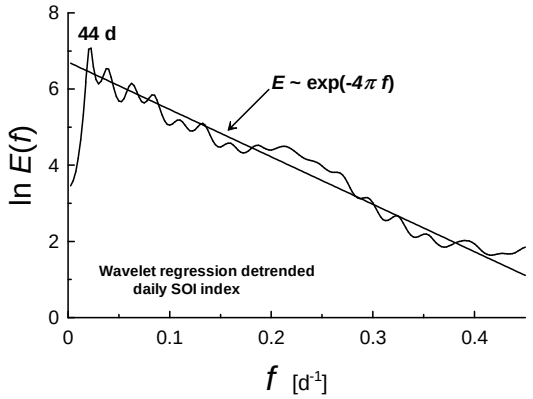

FIG. 4: Spectrum of the wavelet regression detrended SOI data series (the SOI data were taken from Ref. [17]). In the semi-logarithmic scales used in the figure the straight line indicates the exponential decay Eq. (1).

the chaotic exponential decay shown in Fig. 1.

Additionally to the exponential spectrum, let us check the chaotic character of the wavelet regression detrended NAO data set calculating the largest Lyapunov exponent : λ_{max}. A strong indicator for the presence of chaos in the examined time series is condition $\lambda_{max} > 0$. If this is the case, then we have so-called exponential instability. Namely, two arbitrary close trajectories of the system will diverge apart exponentially, that is the hallmark of chaos. To calculate λ_{max} we used a direct algorithm developed by Wolf et al [12]. Figure 3 shows the pertaining average maximal Lyapunov exponent at the pertaining time, calculated for the same data as those used for calculation of the spectrum (Fig. 1). The largest Lyapunov exponent converges very well to a positive value $\lambda_{max} \simeq 0.053d^{-1} > 0$.

In Fig. 1 one can readily recognize a peak corresponding to a pumping period approximately equal to 40 days. It should be noted, that the 40-day oscillations are well known as an intrinsic mode of the Northern Hemisphere extratropics, which is exited presumably due to instabilities related to large-scale topography (see, for instance, Refs. [13]-[15]) In this case the pumping period (40 d) is considerably larger than the daily solar forcing period. Thus, the exponential chaotic decay (Fig. 1) can be considered as a dissipation mechanism for these oscillations.

Another example of the large-scale climate oscillations with the chaotic dissipation mechanism can be recognized in Southern Hemisphere, where one of the most significant and recurrent patterns of atmospheric variability between the western and eastern tropical Pacific is known as Southern Oscillation. The Southern Oscillation is related to the variability of the Walker circulation system: a circulation pattern characterized by sinking air above the eastern Pacific and rising air above the western Pacific. The Southern Oscillation is often considered as the atmospheric component of *El Niño* phenomenon. The daily Southern Oscillation Index (SOI) has been calculated based on the differences in air pressure anomaly between Tahiti and Darwin, Australia [16] for last 20 years [17]. Figure 4 shows a spectrum of the wavelet regression detrended data calculated using the maximum entropy method. A semi-logarithmic plot was used in Fig. 4 in order to show the exponential decay Eq. (1) (cf Fig.1).

I thank to J. Hurrell and to the Department of Environment and Resource Management (Queensland) for sharing their data.

[1] J.P. Gollub, and S. V. Benson, Chaotic response to periodic perturbations of a convecting flow, Phys. Rev. Lett., **41**, 948-951 (1978).
[2] M. Franz, and M. Zhang, Suppression and creation of chaos in a periodically forced Lorenz system. Phys. Rev. E, **52**, 3558-3565 (1995).
[3] N. Ohtomo, K. Tokiwano, Y. Tanaka, A. Sumi, S. Terachi, and H. Konno, Exponential Characteristics of Power Spectral Densities Caused by Chaotic Phenomena, J. Phys. Soc. Jpn. **64** 1104-1113 (1995).
[4] J. D. Farmer, Chaotic attractors of an infinite dimensional dynamic system, Physica D, **4**, 366-393 (1982).
[5] D.E. Sigeti, Survival of deterministic dynamics in the presence of noise and the exponential decay of power spectrum at high frequencies. Phys. Rev. E, **52**, 2443-2457 (1995).
[6] U. Frisch and R. Morf, Intermittency in non-linear dynamics and singularities at complex times, Phys. Rev. **23**, 2673 (1981).
[7] A. Bershadskii, Chaotic climate response to long-term solar forcing variability, EPL (Europhys. Lett.), **88**, 60004 (2009).
[8] J.W. Hurrell et al., An Overview of the North Atlantic Oscillation, in "The North Atlantic Oscillation: Climatic Significance and Environmental Impact", Geophysical Monograph **134**, p.1, American Geophysical Union (2003).
[9] The data are available at http://www.cgd.ucar.edu/cas/jhurrell/indices.html
[10] http://www.cpc.ncep.noaa.gov/products/precip/CWlink/pna/nao_loading.html
[11] T. Ogden, Essential Wavelets for Statistical Applications and Data Analysis (Birkhauser, Basel, 1997).
[12] A. Wolf et al., Determining Lyapunov exponents from a time series, Physica D, **16**, 285 (1985).
[13] V. Magana, The 40-day and 50-day oscillations in atmospheric angular momentum at various latitudes, J. Geophys. Res., **98**, 10441 (1993).
[14] S.L. Marcus, M. Ghil,, and J.O. Dickey, The extratrop-

ical 40-day oscillation in the UCLA General Circulation Model, Part I: Atmospheric angular momentum, J. Atmos. Sci., **51**, 1431 (1994).

[15] M. Ghil, and A.W. Robertson, "Waves" vs. "particles" in the atmosphere's phase space: A pathway to long-range forecasting? Proc. Natl. Acad. Sci., **99** (Suppl. 1), 2493 (2002).

[16] A.J. Troup, The Southern Oscillation. Quart. J. Roy. Met. Soc., **91** 490 (1965).

[17] The data are available at http://www.longpaddock.qld.gov.au/SeasonalClimateOutlook/SouthernOscillationIndex/SOIDataFiles/index.html